Contribution from the Dipartimento di Chimica Inorganica e Metallorganica, Università di Milano, 20133 Milano, Italy, and Department of Chemistry, Northwestern University, Evanston, Illinois 60201

Synthesis and Characterization of Copper(I), Copper(II), Zinc(II), Cobalt(II), and Iron(II) Complexes of a Chelating Ligand Derived from 2,6-Diacetylpyridine and L-Histidine. Oxygenation of the Copper(I), Cobalt(II), and Iron(II) Complexes. Crystal Structure of the Zinc(II) Complex

LUIGI CASELLA,*[1a] MICHAEL E. SILVER,[1b] and JAMES A. IBERS*[1b]

Received April 18, 1983

The synthesis and characterization of the perchlorate salts of the copper(I), copper(II), zinc(II), cobalt(II), and iron(II) complexes of 2,6-bis[1-((1-(carboxymethyl)-2-imidazol-4-ylethyl)imino)ethyl]pyridine = L-bisp (the condensation product of 2,6-diacetylpyridine with two molecules of the methyl ester of the amino acid L-histidine) along with an X-ray structural investigation of the zinc(II) complex, $[Zn(L\text{-bisp})][ClO_4]_2$, are reported. The zinc complex crystallizes in the space group D_2^4-$P2_12_12_1$ four formula units in a cell of dimensions (at −152 °C) a = 28.872 (18) Å, b = 9.567 (6) Å, and c = 10.344 (6) Å. The structure was described by 406 variable parameters, and at convergence the values for R and R_w (on F^2, 5784 data) were 0.060 and 0.090 for the L,L enantiomer. The zinc atom is bonded to five nitrogen atoms and displays a coordination geometry intermediate between a trigonal bipyramid and a square pyramid. Both of the six-membered amino acid chelate rings of the L-bisp ligand adopt the λ configuration. The Cu(I) complex is inert to dioxygen in the solid state but does react with O_2 at ambient conditions in dry acetonitrile. The reaction is complete in ca. 1 h and can be slowly reversed by degassing (N_2) and gentle heating, the degree of reversibility being about 80% for each of several oxy–deoxy cycles. Spectral evidence indicates the oxygenated product is not simply $[Cu(L\text{-bisp})][ClO_4]_2$ and that the L-bisp ligand remains intact. The stoichiometry of the oxygenation reaction is 0.5 mol (±10%) of O_2/mol of copper. Both the Fe(II) and the Co(II) complexes of L-bisp show low or no reactivity to dioxygen in dry acetonitrile or dimethylformamide. However, pyridine solutions of these two complexes do react irreversibly with O_2 at ambient conditions and, in both cases, IR evidence is indicative of concomitant ligand oxidation.

Introduction

The importance of histidyl residues as metal binding sites in biological systems is well recognized.[2] Many of these systems are enzymes and proteins that contain copper and iron as prosthetic groups. They are mostly involved in oxygen transport,[3] metal storage and transport,[4,5] electron transfer,[6,7a] or oxygen activation.[7,8] Although the iron systems often contain heme prosthetic groups, the presence of iron–histidyl centers has been established for the active site of the non-heme oxygen-carrying protein hemerythrin found in certain species of invertebrate phyla.[9] The stoichiometry of oxygen binding of hemerythrin, two metal ions per oxygen molecule, is the same as that of hemocyanin, the non-heme copper protein that functions as the oxygen carrier in the hemolymph of some species of molluscs and arthropods.[10] The interaction of derivatives of histidine with metal ions has been extensively studied, particularly for copper(II).[2a,11] These investigations are in general aimed at establishing correlations between the spectral properties of the complexes and the mode of binding of the potentially tridentate histidine ligand,[12] while imidazole binding in metalloproteins (mostly copper) is usually simulated by nitrogen heterocyclic bases.[13] A difficulty in the study of

(1) (a) Università di Milano. (b) Northwestern University.

(2) (a) Sundberg, R. J.; Martin, R. B. *Chem. Rev.* **1974**, *74*, 471–517. (b) Schneider, F. *Angew. Chem., Int. Ed. Engl.* **1978**, *17*, 583–592. (c) Brill, A. S. "Transition Metals in Biochemistry"; Springer-Verlag: New York, 1977; Chapter 2.

(3) (a) Basolo, F.; Hoffman, B. M.; Ibers, J. A. *Acc. Chem. Res.* **1975**, *8*, 384–392. (b) Collman, J. P. *Ibid.* **1977**, *10*, 265–272. (c) Drago, R. S.; Corden, B. B. *Ibid.* **1980**, *13*, 353–360. (d) Traylor, T. G. *Ibid.* **1981**, *14*, 102–109. (e) Jones, R. D.; Summerville, D. A.; Basolo, F. *Chem. Rev.* **1979**, *79*, 139–179. (f) Smith, T. D.; Pilbrow, J. R. *Coord. Chem. Rev.* **1981**, *39*, 295–383. (g) Buchler, J. W. *Angew. Chem., Int. Ed. Engl.* **1978**, *17*, 407–423.

(4) (a) Lau, S.-J.; Sarkar, B. *J. Biol. Chem.* **1971**, *246*, 5938–5943. (b) Kruck, T. P. A.; Sarkar, B. *Can. J. Chem.* **1973**, *51*, 3549–3554. (c) May, P. M.; Linder, P. W.; Williams, D. R. *J. Chem. Soc., Dalton Trans.* **1977**, 588–595.

(5) (a) Flatmark, T.; Romslo, I. In "Bioinorganic Chemistry"; Raymond, K. N., Ed.; American Chemical Society: Washington, DC, 1977; pp 78–92. (b) Smith, T. D.; Pilbrow, J. R. In "Biological Magnetic Resonance", Berliner, L. J., Reuben, J., Eds.; Plenum Press: New York, 1980; Vol. 2, pp 85–168. (c) Chasteen, N. D. *Coord. Chem. Rev.* **1977**, *22*, 1–36.

(6) Lappin, A. G. *Met. Ions Biol. Syst.* **1981**, *13*, 15–71.

(7) (a) Beinert, H. *Coord. Chem. Rev.* **1980**, *33*, 55–85. (b) Lerch, K. *Met. Ions Biol. Syst.* **1981**, *13*, 143–186. (c) Reinhammar, B.; Malmström, B. G. In "Copper Proteins"; Spiro, T. G., Ed.; Wiley: New York, 1981; pp 109–149.

(8) (a) Matsuura, T. *Tetrahedron* **1977**, *33*, 2869–2905. (b) Jefford, C. W.; Cadby, P. A. *Fortschr. Chem. Org. Naturst.* **1981**, *40*, 191–265. (c) Spiro, T. G., Ed. "Metal Ion Activation of Dioxygen"; Wiley: New York, 1980. (d) Sugiura, Y. *J. Am. Chem. Soc.* **1980**, *102*, 5208–5215.

(9) (a) Kurtz, D. M., Jr.; Shriver, D. F.; Klotz, I. M. *Coord. Chem. Rev.* **1977**, *24*, 145–178. (b) Stenkamp, R. E.; Jensen, L. H. *Adv. Inorg. Biochem.* **1979**, *1*, 219–233. (c) Loehr, J. S.; Loehr, T. M. *Ibid.* **1979**, *1*, 235–252. (d) Elam, W. T.; Stern, E. A.; McCallum, J. D.; Loehr, J. S. *J. Am. Chem. Soc.* **1982**, *104*, 6369–6373. (e) *Ibid.* **1983**, *105*, 1919–1923.

(10) (a) Bannister, J. V., Ed. "Structure and Function of Hemocyanin"; Springer-Verlag: Berlin, 1977. (b) Lamy, J. N., Lamy, J., Eds. "Invertebrate Oxygen-Binding Proteins. Structure, Active Site, and Function"; Marcel Dekker: New York, 1981. (c) Lontie, R.; Witters, R. *Met. Ions Biol. Syst.* **1981**, *13*, 229–258. (d) Solomon, E. I. In "Copper Proteins"; Spiro, T. G., Ed.; Wiley: New York, 1981; pp 41–108.

(11) (a) Sigel, H. *Met. Ions Biol. Syst.* **1973**, *2*, 63–125. (b) Martin, R. B. *Ibid.* **1979**, *9*, 1–39. (c) Chow, S. T.; McAuliffe, C. A. *Prog. Inorg. Chem.* **1975**, *19*, 51–103.

(12) See, for instance: (a) Led, J. J.; Grant, D. M. *J. Am. Chem. Soc.* **1977**, *99*, 5845–5858. (b) Yamauchi, O.; Sakurai, T.; Nakahara, A. *Ibid.* **1979**, *101*, 4164–4172. (c) Camerman, N.; Fawcett, J. K.; Kruck, T. P. A.; Sarkar, B.; Camerman, A. *Ibid.* **1978**, *100*, 2690–2693. (d) Sugiura, Y.; Hirayama, Y. *Ibid.* **1977**, *99*, 1581–1585. (e) Wasylishen, R. E.; Cohen, J. S. *Ibid.* **1977**, *99*, 2480–2482. (f) Sugiura, Y. *Inorg. Chem.* **1978**, *17*, 2176–2182. (g) Sakurai, T.; Nakahara, A. *Ibid.* **1980**, *19*, 847–853. (h) Gulka, R.; Isied, S. S. *Ibid.* **1980**, *19*, 2842–2844. (i) Hoggard, P. E. *Ibid.* **1981**, *20*, 415–420. (j) Casella, L.; Gullotti, M. *Ibid.* **1983**, *22*, 242–249. (k) Nair, M. S.; Santappa, M.; Natarajan, P. *J. Chem. Soc., Dalton Trans.* **1980**, 1312–1316, 2138–2142. (l) Kayali, A.; Berthon, G. *Ibid.* **1980**, 2374–2381. (m) Goodman, B. A.; McPhail, D. B.; Powell, H. K. J. *Ibid.* **1981**, 822–827. (n) Itabashi, M.; Itoh, K. *Bull. Chem. Soc. Jpn.* **1980**, *53*, 3131–3137. (o) Bagger, S. *Acta Chem. Scand., Ser. A* **1980**, *A34*, 63–66 and references therein. (p) Casella, L.; Gullotti, M. *J. Inorg. Biochem.* **1983**, *18*, 19–31.

0020-1669/84/1323-1409$01.50/0

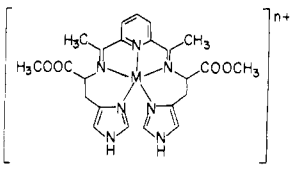

Figure 1. General structure of the M(L-bisp)$^{n+}$ complexes.

simple metal–histidine complexes in solution is the presence of species with mixed chelation modes.[11] This difficulty has been recognized, for instance, in the investigation of the reaction between copper(II)–histidine complexes and superoxide ion[14] and complicates interpretation of the reactions with dioxygen of cobalt(II)–histidine complexes.[2a,11c,15] We have recently shown that when the histidine residue is part of a polydentate Schiff-base ligand it is possible to control the mode of coordination of the amino acid to a metal ion, since this mode is apparently ruled by the chelate ring type of the fused carbonyl residue.[16] As an extension of these studies we report here the synthesis and characterization of the copper(I), copper(II), zinc(II), cobalt(II), and iron(II) complexes of the ligand 2,6-bis[1-((1-(carboxymethyl)-2-imidazol-4-ylethyl)-imino)ethyl]pyridine (=L-bisp) that results from the condensation of 2,6-diacetylpyridine with two molecules of L-histidine methyl ester. We also report a comparison of the reactivity toward dioxygen of Cu(L-bisp)$^+$, Co(L-bisp)$^{2+}$, and Fe(L-bisp)$^{2+}$ and the X-ray structural investigation of a member of this series of compounds, $[Zn(L\text{-bisp})][ClO_4]_2$. The structure of the L-bisp complexes is shown schematically in Figure 1, where the metal is assumed to be five-coordinate. Related copper(I), copper(II), and zinc(II) complexes derived from histamine have been reported recently,[17,18] the Cu(imep)$^+$ complex (imep = 2,6-bis[1-((2-imidazol-4-ylethyl)imino)-ethyl]pyridine) being one of the few copper(I) systems that exhibits some degree of reversible dioxygen binding.[17,19] However, the Cu(imep)$^+$ complex was poorly characterized owing to difficulties with purification.

Experimental Section

All reagents were of the highest grade commercially available. Tetrakis(acetonitrile)copper(I) perchlorate was prepared according to a published procedure.[20] Pyridine (Carlo Erba spectral grade, permanganate resistant) was stored over potassium hydroxide in the dark and distilled under a reduced pressure of nitrogen immediately before use. Acetonitrile (spectral grade) was distilled from potassium permanganate and dry potassium carbonate and then stored over calcium hydride and distilled under nitrogen immediately prior to use. Dimethylformamide was refluxed under vacuum over barium oxide to remove dimethylamine, stored over calcium hydride, and distilled under reduced pressure before use. Deuterated solvents were degassed and stored under nitrogen over molecular sieves (3 Å). The syntheses of all the complexes were carried out under nitrogen in Schlenkware to prevent any possible oxidation. Elemental analyses were from the microanalytical laboratory of the Università di Milano. Infrared spectra were recorded on a Nicolet MX-1E FT-IR instrument; a standard resolution of 2.0 cm^{-1} was used in the measurements. Electronic spectra were recorded on a Beckman DK-2A spectrophotometer. Circular dichroism spectra were recorded on a Jobin-Yvonne Mark III dichrograph, calibrated with a solution of isoandrosterone in dioxane ($\Delta\epsilon$ = +3.31 at 304 nm). The optical and CD spectra of air-sensitive solutions were obtained in 1-cm and 1-mm quartz cells fitted with Schlenk connections. Proton NMR spectra were recorded at 80 MHz on a Bruker WP-80 spectrometer using the pulsed Fourier transform technique. EPR spectra were obtained at X-band frequencies on a Varian E-109 instrument from samples contained in 3-mm quartz tubes fitted with Schlenk connections. Magnetic susceptibilities of solid samples were measured at 295 K by the Faraday technique on a Cahn 1000 electrobalance. Tetrakis(thiocyanato)mercury cobaltate was used as a susceptibility standard, and diamagnetic corrections were estimated by measurements on $[Zn(L\text{-bisp})][ClO_4]_2$ and with use of the appropriate Pascal constants.[21] Conductivity measurements were performed on 10^{-3} M acetonitrile solutions of the complexes with the use of a Philips conductimeter, Model PR 9500. The MS spectra were recorded on a Varian MAT 112 spectrometer at 70 eV.

Preparations of the Complexes. The syntheses of L-bisp complexes were performed according to the following general procedure. L-Histidine methyl ester was freed from its dihydrochloride salt (10.5 mmol) by stirring with the appropriate amount of methanolic ~1 N sodium hydroxide in chloroform (~100 mL). After filtration of the precipitate of sodium chloride, evaporation to dryness under vacuum of the solution gave a light yellow oil. This was dissolved in absolute methanol (~30 mL), and 2,6-diacetylpyridine (5 mmol) was added. The solution was refluxed for a few minutes under nitrogen and then cooled to room temperature. The solid metal perchlorate salt (5 mmol) was quickly added under a stream of nitrogen, and the mixture was refluxed for several hours under nitrogen. The progress of the condensation reaction was checked from time to time by monitoring the decrease of the ketone ν(C=O) band at 1700 cm^{-1} in the IR spectra of small samples of the solution after evaporation to dryness. In general, it was found useful to evaporate the reaction mixture to dryness under vacuum after refluxing for a few hours and then to add a corresponding amount of degassed absolute methanol to the residue. This process removes the water formed in the condensation and accelerates the completion of the reaction. When the amount of free ketone appeared negligible, the mixture was cooled to room temperature and the solid was collected by filtration and dried

(13) See, for instance: (a) Amundsen, A. R.; Whelan, J.; Bosnich, B. *J. Am. Chem. Soc.* **1977**, *99*, 6730–6739. (b) Thompson, J. S.; Marks, T. J.; Ibers, J. A. *Ibid.* **1979**, *101*, 4180–4192. (c) Thompson, J. S.; Sorrell, T.; Marks, T. J.; Ibers, J. A. *Ibid.* **1979**, *101*, 4193–4200. (d) Gagné, R. R.; Allison, J. L.; Gall, R. S.; Koval, C. A. *Ibid.* **1977**, *99*, 7170–7178. (e) Petty, R. H.; Welch, B. R.; Wilson, L. J.; Bottomley, L. A.; Kadish, K. M. *Ibid.* **1980**, *102*, 611–620. (f) Gagné, R. R.; Kreh, R. P.; Dodge, J. A. *Ibid.* **1979**, *101*, 6917–6927. (g) McKee, V.; Dagdigian, J. V.; Bau, R.; Reed, C. A. *Ibid.* **1981**, *103*, 7000–7001. (h) Sorrell, T. N.; Jameson, D. L. *Ibid.* **1982**, *104*, 2053–2054. (i) Karlin, K. D.; Gultneh, Y.; Hutchinson, J. P.; Zubieta, J. *Ibid.* **1982**, *104*, 5240–5242. (j) Hendriks, H. M. J.; Birker, P. J. M. W. L.; van Rijn, J.; Verschoor, G. C.; Reedijk, J. *Ibid.* **1982**, *104*, 3607–3617. (k) Karlin, K. D.; Dahlstrom, P. L.; Cozzette, S. N.; Scensny, P. M.; Zubieta, J. *J. Chem. Soc., Chem. Commun.* **1981**, 881–882. (l) Burnett, M. G.; McKee, V.; Nelson, S. M.; Drew, M. G. B. *Ibid.* **1980**, 829–831. (m) Burnett, M. G.; McKee, V.; Nelson, S. M. *Ibid.* **1980**, 599–601. (n) Gagné, R. R.; Gall, R. S.; Lisensky, G. C.; Marsh, R. E.; Speltz, L. M. *Inorg. Chem.* **1979**, *18*, 771–781. (o) Gagné, R. R.; Kreh, R. P.; Dodge, J. A.; Marsh, R. E.; McCool, M. *Ibid.* **1982**, *21*, 254–261. (p) Sorrell, T. N.; Malachowski, M. R.; Jameson, D. L. *Ibid.* **1982**, *21*, 3250–3252. (q) Dedert, P. L.; Thompson, J. S.; Ibers, J. A.; Marks, T. J. *Ibid.* **1982**, *21*, 969–977. (r) Dedert, P. L.; Sorrell, T.; Marks, T. J.; Ibers, J. A. *Ibid.* **1982**, *21*, 3506–3517. (s) Takano, S.; Yano, Y.; Takagi, W. *Chem. Lett.* **1981**, 1177–1180. (t) Suzuki, M.; Kanatomi, H.; Murase, I. *Ibid.* **1981**, 1745–1748. (u) Ortego, J. D.; Seymour, M. *Polyhedron* **1982**, *1*, 21–30. (v) Sakurai, T.; Kaji, H.; Nakahara, A. *Inorg. Chim. Acta* **1982**, *67*, 1–5.

(14) Weinstein, J.; Bielski, B. H. J. *J. Am. Chem. Soc.* **1980**, *102*, 4916–4919.

(15) (a) Michailidis, M. S.; Martin, R. B. *J. Am. Chem. Soc.* **1969**, *91*, 4683–4689. (b) Morris, P. J.; Martin, R. B. *Ibid.* **1970**, *92*, 1543–1546. (c) Zompa, L. J. *J. Chem. Soc. D* **1969**, 783. (d) Bagger, S.; Gibson, K.; Sørensen, C. S. *Acta Chem. Scand.* **1972**, *26*, 2503–2510. (e) Bagger, S.; Gibson, K. *Ibid.* **1972**, *26*, 3788–3796. (f) Gillard, R. D. *Inorg. Chim. Acta, Rev.* **1967**, *1*, 69–86. (g) McLendon, G.; Martell, A. E. *Coord. Chem. Rev.* **1976**, *19*, 1–39. (h) Watters, K. L.; Wilkins, R. G. *Inorg. Chem.* **1974**, *13*, 752–753.

(16) (a) Casella, L.; Gullotti, M. *Inorg. Chem.* **1981**, *20*, 1306–1308. (b) Casella, L.; Gullotti, M. *J. Am. Chem. Soc.* **1981**, *103*, 6338–6347. (c) Casella, L.; Gullotti, M.; Pacchioni, G. *Ibid.* **1982**, *104*, 2386–2396. (d) Casella, L.; Gullotti, M. *Inorg. Chem.* **1983**, *22*, 2259–2266.

(17) (a) Simmons, M. G.; Wilson, L. J. *J. Chem. Soc., Chem. Commun.* **1978**, 634–636. (b) Simmons, M. G.; Merrill, C. L.; Wilson, L. J.; Bottomley, L. A.; Kadish, K. M. *J. Chem. Soc., Dalton Trans.* **1980**, 1827–1837.

(18) Korp, J. D.; Bernal, I.; Merrill, C. L.; Wilson, L. J. *J. Chem. Soc., Dalton Trans.* **1981**, 1951–1956.

(19) (a) Kim, S. J.; Takizawa, T. *J. Chem. Soc., Chem. Commun.* **1974**, 356–357. (b) Bulkowski, J. E.; Burk, P. L.; Ludmann, M.-F.; Osborn, J. A. *Ibid.* **1977**, 498–499. (c) Nishida, Y.; Takahashi, K.; Kuramoto, H.; Kida, S. *Inorg. Chim. Acta* **1981**, *54*, L103–L104. (d) Cited in: Kwik, W.-L.; Ang, K.-P. *J. Chem. Soc., Dalton Trans.* **1981**, 452–455.

(20) Hemmerich, P.; Sigwart, C. *Experientia* **1963**, *19*, 488–489.

(21) Mabbs, F. E.; Machin, D. J. "Magnetism and Transition Metal Complexes"; Chapman and Hall: London, 1974; Chapter 1.

under vacuum. Yields ranged between 40 and 70%. The copper(I), zinc(II), and iron(II) complexes were recrystallized from degassed absolute methanol, while the copper(II) and the cobalt(II) complexes were more conveniently recrystallized from degassed absolute ethanol and ethanol–benzene (8:2 v:v), respectively.

[Cu(L-bisp)][ClO$_4$]. Anal. Calcd for $C_{23}H_{27}ClCuN_7O_8$: C, 43.94; H, 4.33; N, 15.60. Found: C, 43.60; H, 4.44; N, 15.39. Complete IR data (Nujol mull, cm^{-1}): 3321 s, 3282 s, 3142 w, 3126 w, 1732 vs, 1618 w, 1601 vw, 1581 m, 1556 vw, 1494 w, 1403 w, 1347 w, 1334 w, 1303 w, 1278 s, 1265 m, 1250 w, 1229 s, 1192 w, 1179 w, 1149 w, 1122 s, 1101 s, 1080 s, 1058 s, 1027 m, 1002 w, 981 w, 967 w, 931 w, 907 vw, 867 vw, 814 m, 767 vw, 750 m, 724 w, 710 w, 684 w, 669 w, 623 s. Λ_M = 135 S cm^2 mol^{-1}. UV–vis (CH_3CN; λ_{max}, nm (ϵ)): 563 (1250), 376 (2700), 275 sh (9000), 260 (11 000), 214 sh (31 000).

[Zn(L-bisp)][ClO$_4$]$_2$. Anal. Calcd for $C_{23}H_{27}Cl_2N_7O_{12}Zn$: C, 37.85; H, 3.73; N, 13.44. Found: C, 37.54; H, 3.77; N, 13.26. Complete IR data (Nujol mull, cm^{-1}): 3360 m, 3310 m, 3132 w, 1753 s, 1732 s, 1638 m, 1590 m, 1503 m, 1354 w, 1326 w, 1296 m, 1272 m, 1261 w, 1232 m, 1204 m, 1173 m, 1100 vs, br, 1033 s, 975 vw, 929 w, 870 vw, 853 w, 821 m, 797 vw, 788 vw, 745 m, 739 m, 722 w, 693 vw, 660 vw, 646 vw, 621 s. Λ_M = 290 S cm^2 mol^{-1}. UV (CH_3CN; λ_{max}, nm (ϵ)): 305 sh (4750), 296 (5400), 275 sh (3700), 250 sh (10 600), 242 sh (13 200), 237 (13 600), 211 (32 000). CD (CH_3CN; λ_{max} nm ($\Delta\epsilon$)): 313 (−8.73), 276 (−10.32), 240 sh (−6.74), 225 (−25.14).

Upon slow evaporation of a 1:1 methanol–ethanol solution of this product crystals suitable for X-ray diffraction study were obtained. These exhibit an identical UV spectrum but larger molar CD extinction coefficients (λ_{max}, nm ($\Delta\epsilon$)): 313 (−10.84), 276 (−12.34), 240 sh (−7.47), 225 (−29.91).

[Cu(L-bisp)][ClO$_4$]$_2$·C$_2$H$_5$OH. Anal. Calcd for $C_{23}H_{27}Cl_2CuN_7O_{12}\cdot C_2H_5OH$: C, 38.79; H, 4.30; N, 12.67. Found: C, 39.10; H, 4.34; N, 12.88. Complete IR data (Nujol mull, cm^{-1}): 3548 m, 3307 m, 3280 m, 3136 m, 1734 s, 1648 sh, 1629 m, 1588 m, 1501 w, 1271 m, 1233 m, 1213 m, 1178 vw, 1100 vs, br, 962 vw, 930 w, 817 w, 776 vw, 753 vw, 721 vw, 623 s. μ_{eff} = 1.83 μ_B. UV–vis (CH_3CN; λ_{max}, nm (ϵ)): 600 sh (400), 450 sh (1000), 350 sh (2800), 285 (5700), 214 (28 500). CD (CH_3CN; λ_{max}, nm ($\Delta\epsilon$)): 660 (+0.03), 580 (−0.04), 360 (−0.03, br), 310 (−0.28).

[Co(L-bisp)][ClO$_4$]$_2$. Anal. Calcd for $C_{23}H_{27}CoCl_2N_7O_{12}$: C, 38.19; H, 3.76; N, 13.56. Found: C, 38.69; H, 3.91; N, 13.76. Complete IR data (Nujol mull, cm^{-1}): 3365 w, 3308 m, 3129 w, 3080 vw, 1753 s, 1733 s, 1625 m, 1589 m, 1498 m, 1353 w, 1325 w, 1293 m, 1269 m, 1261 w, 1232 m, 1203 m, 1173 m, 1095 vs, br, 1034 s, 1021 sh, 1015 sh, 933 w, 928 w, 873 vw, 855 w, 821 m, 797 vw, 786 vw, 746 m, 738 m, 723 w, 695 vw, 660 vw, 647 vw, 624 s. μ_{eff} = 4.28 μ_B. Λ_M = 280 S cm^2 mol^{-1}. UV–vis (CH_3CN; λ_{max}, nm (ϵ)): 1400–1800 (~10), 735 (14), 548 (45), 482 (64), 410 sh (220), 380 sh (440), 315 sh (4200), 304 (5200), 297 sh (5000), 235 sh (20 000), 210 (34 000). CD (CH_3CN; λ_{max}, nm ($\Delta\epsilon$)): 750 (−0.25), 598 (−0.32), 575 sh (−0.25), 495 (+0.83), 440 sh (−0.37), 415 sh (−0.94), 385 (−1.72), 360 sh (−1.50), 300 sh (−4.48), 256 (−10.92), 223 (−18.10).

[Fe(L-bisp)][ClO$_4$]$_2$·CH$_3$OH. Anal. Calcd for $C_{23}H_{27}Cl_2FeN_7O_{12}\cdot CH_3OH$: C, 38.31; H, 4.15; N, 13.03. Found: C, 38.71; H, 4.07; N, 12.83. Complete IR data (Nujol mull, cm^{-1}): 3585 m, 3296 s, 3144 vw, 3126 w, 1745 s, 1632 m, 1589 m, 1502 w, 1358 m, 1341 w, 1322 vw, 1277 m, 1272 m, 1256 w, 1230 vw, 1205 s, 1176 s, 1100 vs, br, 1027 w, 1010 w, 977 vw, 962 vw, 932 w, 879 vw, 862 vw, 810 m, 773 vw, 763 vw, 736 w, 721 vw, 697 vw, 687 vw, 682 vw, 625 s. μ_{eff} = 5.02 μ_B. Λ_M = 255 S cm^2 mol^{-1}. UV–vis (CH_3CN; λ_{max}, nm (ϵ)): 765 sh (280), 625 sh (1300), 570 sh (1700), 513 (2950), 360 sh (370), 310 sh (5700), 300 (7000), 238 sh (21 000), 210 (30 000).

Manometric Oxygen-Uptake Measurements. A thermostated three-necked flask connected to a thermostated gas microburet (5 cm^3, filled with dry oxygen) was fitted with a spoon-shaped glass stopper. A known volume of degassed solvent (30–40 mL) was poured into the flask and saturated with dry oxygen under stirring. A solid sample weighing 100–150 mg was placed on the spoon, and this was fitted to the side arm of the flask under a stream of oxygen. After equilibration to constant temperature, the gas buret was filled with oxygen and the spoon was turned upside down, causing the solid to fall into the solvent. Vigorous stirring was maintained throughout the experiment to ensure rapid equilibration. The volume of oxygen absorbed by the solution was then measured from time to time, after further equilibration at atmospheric pressure of the oxygen contained in the buret by means of a Mariotte connected to it.

Table I. Summary of Crystal Data and Intensity Collection

formula	$C_{23}H_{27}Cl_2N_7O_{12}Zn$
fw	729.79
a (at −152 °C)	28.872 (18) Å
b	9.567 (6) Å
c	10.344 (6) Å
V	2857 Å^3
Z	4
density (calcd for −152 °C)	1.697 g cm^{-3}
density (measd in $CHBr_3$–hexane)	1.65 (2) g cm^{-3}
space group	D_2^4 – $P2_12_12_1$
cryst dimens	0.20 × 0.31 × 0.49 mm
boundary faces of cryst	{100}, {010} ($\bar{1}01$), ($\bar{3}0\bar{1}$), ($\bar{2}01$), (001)
temp	−152 °C[a]
radiation	Mo Kα (λ(Mo Kα_1) = 0.7093 Å), graphite monochromated
linear abs coeff	10.96 cm^{-1}
transmission factors	0.785–0.842
receiving aperture	3.1 × 5.2 mm; 34 cm from crystal
take-off angle	2.7°
scan speed	2° in 2θ/min
scan range	0.60° below Kα_1 to 0.85° above Kα_2
bkgd counts	10 s at each end of scan, with rescan option[b]
2θ limits	3.5–65.0°
final no. of variables	406
data collected	$+h,k,l$
unique data	5784
unique data with $F_o^2 > 3\sigma(F_o^2)$	4848

[a] The low-temperature system is based on a design by: Huffman, J. C. Ph.D. Thesis, Indiana University, 1974. [b] Lenhert, P. G. *J. Appl. Crystallogr.* **1975**, *8*, 568–570.

Crystallographic Study of [Zn(L-bisp)][ClO$_4$]$_2$. Symmetry and systematic absences consistent with the orthorhombic space group D_2^4-$P2_12_12_1$ were observed by precession and Weissenberg photography. Accurate cell dimensions were obtained by least-squares refinement of the setting angles of 15 computer-centered reflections that had been chosen from diverse regions of reciprocal space with 25° ≤ 2θ(Mo) ≤ 30°. These cell constants and other pertinent data are shown in Table I. Intensity data were collected at −152 °C on a computer-controlled Picker four-circle diffractometer. A total of 5818 intensities were recorded out to 2θ(Mo) = 65.0°. The data were processed as previously described[22] with the use of a value of p of 0.03. The 4848 unique reflections having $F_o^2 > 3\sigma(F_o^2)$ were used in subsequent calculations, and the function minimized was $\sum w(|F_o| - |F_c|)^2$. For the last cycle of refinement all the data were used and the function minimized was $\sum w(F_o^2 - F_c^2)^2$. An absorption correction was applied to the data.[23]

The structure was solved by standard Patterson and Fourier methods and refined by full-matrix least-squares techniques.[23] Values of the atomic scattering factors[24] and the anomalous terms[25] were from the usual sources. The effects of anomalous dispersion for the Zn and Cl atoms were included in F_c.[26] Refinement of an anisotropic model consisting of all 45 non-hydrogen atoms converged to values of R and

(22) See, for example: Waters, J. M.; Ibers, J. A. *Inorg. Chem.* **1977**, *16*, 3273–3277.
(23) The Northwestern absorption program, AGNOST, includes both the Coppens–Leiserowitz–Rabinovich logic for Gaussian integration and the Tompa–de Meulenaer analytical method. In addition to various local programs for the CDC 6600 and the Harris 800 computers, modified versions of the following were employed: Zalkin's FORDAP Fourier summation program; Johnson's ORTEP thermal ellipsoid plotting program; Busing's and Levy's ORFFE error function program. Our full-matrix least-squares program, NUCLS, in its nongroup form closely resembles the Busing–Levy ORFLS program.
(24) Cromer, D. T.; Waber, J. T. "International Tables for X-ray Crystallography"; Kynoch Press: Birmingham, England, 1974; Vol. IV, Table 2.2A. Cromer, D. T. *Ibid.*, Table 2.3.1.
(25) Stewart, R. F.; Davidson, E. R.; Simpson, W. T. *J. Chem. Phys.* **1965**, *42*, 3175–3187.
(26) Ibers, J. A.; Hamilton, W. C. *Acta Crystallogr.* **1964**, *17*, 781–782.

Figure 2. Stereodiagram of the unit cell for $[Zn(L\text{-bisp})][ClO_4]_2$. The two crystallographically independent perchlorate ions are labeled A and B. The view is approximately down the *b* axis; the *c* axis is vertical.

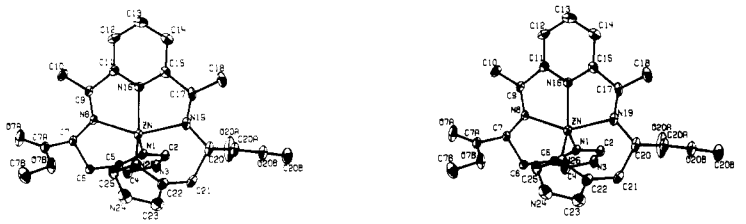

Figure 3. Stereodiagram of the $[Zn(L\text{-bisp})]^{2+}$ cation showing the atom-labeling scheme. Ellipsoids are drawn at the 50% probability level. Hydrogen atoms are omitted for clarity.

R_w of 0.0680 and 0.0772 for the D,D enantiomer and 0.0499 and 0.0603 for the expected L,L enantiomer, respectively.

A difference electron density map revealed the positions of all the 27 H atoms. The hydrogen atoms were then included at their calculated idealized positions as a fixed contribution to F_c. A C–H separation of 0.95 Å was assumed. The thermal parameter for a hydrogen atom was fixed at 1.0 Å^2 greater than the equivalent isotropic thermal parameter of its attached carbon atom.

The final values for R and R_w on F^2 are 0.060 and 0.090, respectively, and the standard error in an observation of unit weight is 1.37 e^2. For the portion of the data having $F_o^2 > 3\sigma(F_o^2)$ the conventional values of R and R_w on F are 0.041 and 0.043. The final difference electron density is essentially featureless, with the largest peak having a height of 1.38 (12) e Å^{-3}.

Final atomic coordinates and thermal parameters for the nonhydrogen atoms are listed in Tables II and III,[27] respectively. Hydrogen atom parameters are given in Table IV.[27] Table V lists the value of $10|F_o|$ vs. $10|F_c|$.[27]

Results and Discussion

Synthesis of the Complexes. The L-bisp complexes were obtained by metal ion template condensation of 2,6-diacetylpyridine and two molecules of L-histidine methyl ester. The free ligand was not isolated since preliminary experiments[28] have shown that the reaction between diacetylpyridine and L-histidine methyl ester or histamine in the presence of triethylamine gives products contaminated by the cyclic tetrahydropyridine derivatives formed by cyclization of the Schiff bases.[16b]

Structure of $[Zn(L\text{-bisp})][ClO_4]_2$. Crystals of $[Zn(L\text{-bisp})][ClO_4]_2$ suitable for diffraction study were obtained from slow evaporation of a 1:1 methanol–ethanol solution. The crystal structure consists of the packing of four molecules of the L,L enantiomer of the zinc complex and eight perchlorate ions in the unit cell. A stereo drawing of the cell is shown in Figure 2. There are two intermolecular distances that are at least 0.2 Å shorter than the appropriate van der Waals contacts[29] (both involving methyl carbon C(10) with the pyridine ring; C(10)–C(13) = 3.28 Å, C(10)–C(14) = 3.50 Å). Three other intermolecular distances are approximately 0.1 Å shorter than the appropriate van der Waals contact (N(24)–O(2A) = 2.99 Å, N(3)–O(7A) = 3.00 Å, and N(3)–O(1A) = 3.03 Å). The labeling scheme for this complex is shown in Figure 3. The two independent perchlorate ions are referred to as A and B.

Table II. Positional Parameters[a] for the Non-Hydrogen Atoms of $[Zn(L\text{-bisp})][ClO_4]_2$

atom	*x*	*y*	*z*
Zn	−0.130 899 (12)	−0.175 004 (36)	0.238 894 (31)
N1	−0.104 796 (94)	−0.071 14 (27)	0.088 29 (25)
C2	−0.113 52 (12)	0.055 93 (34)	0.040 71 (31)
N3	−0.092 64 (10)	0.071 43 (29)	−0.072 44 (27)
C4	−0.068 67 (12)	−0.049 91 (37)	−0.100 09 (33)
C5	−0.076 61 (11)	−0.137 56 (32)	−0.000 40 (30)
C6	−0.057 09 (11)	−0.280 02 (34)	0.026 19 (32)
C7	−0.092 14 (11)	−0.400 09 (31)	0.030 35 (31)
C7A	−0.069 82 (12)	−0.531 92 (33)	0.085 19 (33)
O7A	−0.071 68 (11)	−0.644 79 (27)	0.036 57 (28)
O7B	−0.048 059 (92)	−0.504 09 (25)	0.196 09 (25)
C7B	−0.025 01 (13)	−0.621 11 (40)	0.257 04 (41)
N8	−0.131 550 (91)	−0.359 26 (25)	0.112 71 (23)
C9	−0.171 32 (11)	−0.416 47 (32)	0.096 52 (31)
C10	−0.183 10 (13)	−0.535 88 (39)	0.009 17 (35)
C11	−0.210 28 (10)	−0.350 86 (33)	0.170 98 (30)
C12	−0.255 97 (11)	−0.395 70 (37)	0.167 40 (34)
C13	−0.288 92 (10)	−0.318 27 (40)	0.232 54 (32)
C14	−0.275 87 (11)	−0.201 24 (37)	0.303 08 (33)
C15	−0.229 11 (10)	−0.164 53 (35)	0.307 55 (29)
N16	−0.198 069 (82)	−0.238 26 (26)	0.240 96 (26)
C17	−0.209 80 (12)	−0.044 39 (33)	0.382 43 (30)
C18	−0.240 07 (13)	0.029 84 (39)	0.476 36 (36)
N19	−0.166 923 (98)	−0.018 83 (27)	0.357 66 (26)
C20	−0.141 57 (12)	0.088 35 (33)	0.429 69 (31)
C20A	−0.152 63 (13)	0.232 66 (36)	0.374 76 (33)
O20A	−0.152 22 (14)	0.260 81 (30)	0.263 20 (27)
O20B	−0.160 245 (84)	0.324 27 (25)	0.467 21 (22)
C20B	−0.167 21 (16)	0.467 17 (39)	0.425 92 (40)
C21	−0.089 08 (12)	0.064 99 (34)	0.411 97 (32)
C22	−0.073 80 (12)	−0.077 73 (36)	0.453 49 (32)
C23	−0.045 68 (13)	−0.114 33 (42)	0.553 32 (35)
N24	−0.043 27 (11)	−0.258 99 (35)	0.551 31 (29)
C25	−0.068 84 (12)	−0.304 14 (36)	0.451 91 (33)
N26	−0.087 676 (91)	−0.198 05 (26)	0.388 21 (25)
ClA	−0.444 694 (25)	−0.357 563 (76)	0.194 898 (70)
ClB	−0.188 250 (45)	−0.246 14 (11)	−0.287 230 (99)
O1A	−0.400 212 (71)	−0.317 46 (26)	0.244 59 (25)
O2A	−0.477 608 (79)	−0.248 50 (25)	0.225 41 (24)
O3A	−0.459 861 (81)	−0.487 35 (23)	0.251 50 (25)
O4A	−0.441 820 (96)	−0.374 46 (27)	0.056 29 (23)
O1B	−0.210 32 (13)	−0.269 52 (34)	−0.410 46 (34)
O2B	−0.220 39 (21)	−0.290 27 (44)	−0.190 27 (45)
O3B	−0.177 96 (13)	−0.101 36 (33)	−0.273 14 (40)
O4B	−0.148 63 (15)	−0.332 33 (45)	−0.280 41 (44)

[a] Estimated standard deviations in the last significant figure(s) are given in parentheses in this table.

The structure of $[Zn(L\text{-bisp})][ClO_4]_2$ is essentially identical with that of $[Zn(imep)][ClO_4]_2$,[18] the only major difference being substitution of a $COO(CH_3)$ ester group for a hydrogen atom on carbon atoms C(7) and C(20). Such a substitution, while having little effect on the structure, results in both C(7)

(27) Supplementary material.
(28) Casella, L.; Ibers, J. A., unpublished results.
(29) We take the van der Waals radii of imidazole NH, pyridyl CH, methyl, and oxygen to be 1.7, 1.7, 2.0, and 1.5 Å, respectively.[30]
(30) Pauling, L. "The Nature of the Chemical Bond", 3rd ed.; Cornell University Press: Ithaca, NY, 1960; p 260.

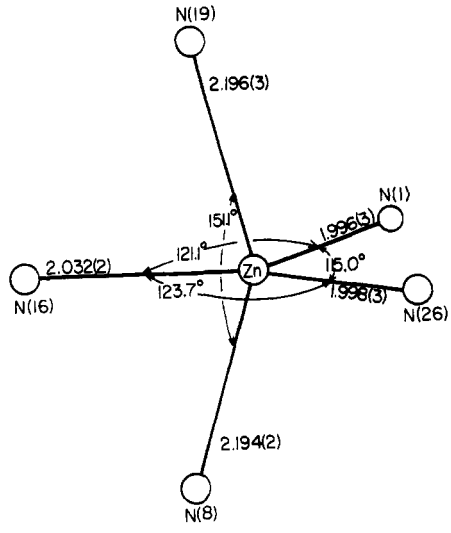

Figure 4. Bond angles and distances within the inner coordination sphere of the $[Zn(L\text{-bisp})]^{2+}$ cation.

and C(20) being chiral centers. Refinement of both the L,L and the D,D enantiomers as described in the Experimental Section resulted in assignment of the L absolute configuration about both of the chiral carbon atoms. This result was expected since L-bisp is the Schiff base condensation product of 2,6-diacetylpyridine with two molecules of the methyl ester of L-histidine.

As in $[Zn(imep)][ClO_4]_2$ and $[Cu(imep)][ClO_4]_2$,[18] the metal atom in $[Zn(L\text{-bisp})][ClO_4]_2$ is bonded to five nitrogen atoms and displays a coordination geometry best described as intermediate between a trigonal bipyramid and a square pyramid (Figure 4). Angles and bond lengths within the inner coordination sphere of $[Zn(L\text{-bisp})][ClO_4]_2$ differ from those of $[Zn(imep)][ClO_4]_2$ by an average of 2.3° and 0.018 Å and by a maximum of 6.1° and 0.035 Å, respectively. Note that the L-bisp structure was based on data collected at −152 °C while the imep structures are based on room-temperature data. Bond distances and angles in the coordination sphere of $[Zn(L\text{-bisp})][ClO_4]_2$ are listed in Table VI.[27]

The carbon–carbon and carbon–nitrogen distances of homologous bonds in $[Zn(L\text{-bisp})][ClO_4]_2$ and $[Zn(imep)][ClO_4]_2$ are all within an average of 0.014 Å of each other, the maximum deviation being 0.036 Å for C(11)–C(12) and C(23)–N(24). The pyridyl ring and both imidazole rings (atoms N(1)–C(5) and atoms C(22)–N(26)) are planar; average displacements from the least-squares planes are 0.011 (3), 0.002 (3), and 0.006 (3) Å, respectively. Selected least-squares planes are presented in Table VII.[27] A shortening in the attachment of the imidazole rings to the ethane bridges at C(5)–C(6) and C(21)–C(22) and a larger than typical[18,31] C–N–C angle in the pyridine ring occurs as it does in both imep structures. If the ester groups on atoms C(7) and C(20) are disregarded, there is more nearly a twofold (C_2) axis of symmetry running through the center of the ligand along the C(13)···N(16) vector than there is for either imep structure. The orientation of the two imidazole rings with respect to the diacetylpyridine plane (atoms N(8), N(16), C(12)–C(15), Table VII[27]) differs by 3.6° for the present structure as compared with 16° for $[Zn(imep)][ClO_4]_2$ and 24° for $[Cu(imep)][ClO_4]_2$. Just as for both imep structures, there is no evidence from observed bond lengths for conjugation from atoms N(8) through C(9) or atoms N(19) through C(17) across to the pyridine ring. The bond distances and angles within the methyl ester groups attached to carbon atoms C(7) and C(20) are typical of values found in other structures containing this function.[32-34] The only significant difference between the two ester groups is in the thermal motion associated with oxygen atoms O(7A) and O(20A), the values of their isotropic thermal parameters being 2.9 and 4.5 $Å^2$, respectively. However, atom O(7A) is involved in a relatively short intermolecular contact whereas atom O(20A) is not.

As this was the first Schiff-base complex of histidine to be structurally characterized, it was of interest to determine the conformation adopted by the six-membered amino acid chelate rings (i.e., atoms N(1)C(5)C(6)C(7)N(8)Zn, ring 1; atoms N(26)C(22)C(21)C(20)N(19)Zn, ring 2). Both rings can be described as cyclohexene boats, but with the C–N edges of their basal planes slightly twisted in opposite directions about an axis connecting the midpoints of these edges. In both cases this twisting results in the ring having left-handed helicity and therefore the λ configuration. However, ring 1 is twisted to a larger extent than ring 2, the angle between the projections of the C–N edges onto a plane that is perpendicular to the basal plane and contains the flagpole atoms (Zn and C(6) or C(21)) being 10.0° for ring 1 and 1.0° for ring 2. In $[Zn(imep)][ClO_4]_2$ both rings are also slightly twisted boats of λ configuration, ring 1 and ring 2 being twisted by 3.1 and 2.8°, respectively. While the cyclohexene-boat configuration results from the imidazole ring being fused to one of the C–N edges, the slight twisting to the λ configuration is most probably a result of crystal-packing forces. As previously mentioned, oxygen atoms O(1A) and O(2A) of perchlorate ion A and atom O(7A) of one of the ester groups make slightly repulsive contacts with the N–H portions of both imidazole rings. Twisting to the λ configuration minimizes these repulsions. Of these three contacts, two involve chelate ring 1, which might account for it being the more twisted of the rings.

Bond lengths and angles for the two independent perchlorate ions are in excellent agreement with literature results.[18,35,36] As previously mentioned, two of the oxygen atoms of perchlorate ion A are within van der Waals contact of the N–H portions of the imidazole rings, while none of the oxygen atoms of perchlorate ion B make any close contacts with other atoms. This is consistent with perchlorate ion B having the larger thermal parameters (the average isotropic thermal parameter for oxygen in perchlorate ions A and B are 2.12 and 6.13 $Å^2$, respectively).

Characterization and Spectral Data. Although only the zinc(II)– and cobalt(II)–L-bisp complexes actually display significant optical activity, we use the abbreviation L-bisp for the ligand to indicate that the L enantiomer of the amino ester was employed in the synthesis of the complexes. The copper(I)–, copper(II)–, and iron(II)–L-bisp complexes, therefore, consist of mixtures of diastereoisomers formed by epimerization of the L-histidine chiral center during the preparation of the complexes. Racemization at the α-carbon atom of complexes of L-histidine Schiff bases is a relatively easy process when the α-C–H bond of the amino acid residue is oriented in a pseudoaxial position and the carboxylate group is pseudoequatorial, i.e. when the chelate ring of the histamine-like bound amino acid residue is in a λ conformation.[16c,d] As observed in the structure of $[Zn(L\text{-bisp})][ClO_4]_2$, this conformation of the L-histidine chelate ring is clearly readily

(31) Bak, B.; Hansen-Nygaard, L.; Rastrup-Andersen, J. *J. Mol. Spectrosc.* **1958**, *2*, 361–368.
(32) Weber, H. P.; Troxler, F. *Helv. Chim. Acta* **1974**, *57*, 2364–2368.
(33) Flippen, J. L. *Acta Crystallogr., Sect. B: Struct. Crystallogr. Cryst. Chem.* **1978**, *B34*, 995–997.
(34) Cameron, A. F.; McElhatton, J.; Campbell, M. M.; Johnson, G. *Acta Crystallogr., Sect. B: Struct. Crystallogr. Cryst. Chem.* **1979**, *B35*, 1263–1266.
(35) Dickens, B. *Acta Crystallogr., Sect. B: Struct. Crystallogr. Cryst. Chem.* **1969**, *B25*, 1875–1882.
(36) Kadooka, M. M.; Warner, L. G.; Seff, K. *J. Am. Chem. Soc.* **1976**, *98*, 7569–7578.

accessible to the L-bisp complexes and it can therefore be anticipated that they would racemize easily. Pyridine solutions of either [Zn(L-bisp)][ClO_4]$_2$ or [Co(L-bisp)][ClO_4]$_2$ (the latter under nitrogen) show, in fact, a progressive decrease of optical activity with time, without appreciable displacement of the CD extrema. The loss of the optical activity of these pyridine solutions is complete within about 1 day (Co(L-bisp)$^{2+}$) or a few days (Zn(L-bisp)$^{2+}$) at room temperature (Figure 5).[27]

The Schiff-base structure of the ligand in all L-bisp complexes is confirmed by imine ν(C=N) bands between ~1620 and ~1640 cm^{-1} in the IR spectra of the complexes, while completely absent are IR bands at 1700 cm^{-1} or at 3200–3400 cm^{-1} attributable to unreacted carbonyl or primary amine functions of the precursors. Typical IR absorptions associated with imidazole nuclei of the histidine residues occur near 3300 (ν(NH)), 3130 (ν(CH)), and 1500 cm^{-1} (ν(ring)).[16b-d] The position of the ν(C=O) stretch of methyl ester groups (1730–1750 cm^{-1}) and the broad feature generally exhibited by the perchlorate ion absorptions near 1100 cm^{-1} indicate that these groups are noncoordinated.[37] Some splitting of the ~1100-cm^{-1} perchlorate IR band in the spectrum of [Cu(L-bisp)][ClO_4] may indicate a slight reduction in the T_d symmetry of the free ion, perhaps as a result of a hydrogen-bonding interaction with the N–H groups of the ligand, as is observed for one of the perchlorate ions in [Zn(L-bisp)][ClO_4]$_2$. Interestingly, the IR spectra of [Zn(L-bisp)][ClO_4]$_2$ and [Co(L-bisp)][ClO_4]$_2$ show two carbonyl stretching bands. This splitting probably reflects the nonequivalence of the ester groups of the ligand, as occurs in the structure of [Zn(L-bisp)][ClO_4]$_2$. Moreover, the overall features of the IR spectra of the zinc(II) and cobalt(II) complexes are almost superimposable, indicating that these chelates may have closely related structures. The IR spectra of the copper(II)- and iron(II)-L-bisp complexes show additional bands in the region 3550–3600 cm^{-1}, attributable to molecules of the alcohol used in the recrystallization of the complexes. The broad features of these bands indicate that the the solvent molecules are not coordinated to the metal centers of the complexes.

As expected, [Cu(L-bisp)][ClO_4] is diamagnetic and its proton NMR spectrum in CD_3CN solution shows the presence of two methyl ester signals (at δ 3.73 and 3.83) and two CH_3C=N signals (at δ 2.12 and 2.34) of equal intensity. Proton signals attributable to nonequivalent imidazole and α-CH groups are also apparent in the spectrum (Figure 6).[27] The nonequivalence of the various proton group signals most probably arises from the presence of different isomers of the compound formed by epimerization of the L-histidine α-carbon atoms during the preparation of the complex.[38] By contrast, the proton NMR spectrum of [Zn(L-bisp)][ClO_4]$_2$ in CD_3CN solution shows the presence of a single set of resonances for the methyl ester (δ 3.88), CH_3C=N (δ 2.53), α-CH (δ 4.80), and imidazole CH (δ 7.21 and 7.87) protons (Figure 7).[27,38] Conductivity data for the complexes measured in acetonitrile solution at 10^{-3} M concentration show that [Cu(L-bisp)][ClO_4] behaves as a 1:1 electrolyte, while the complexes derived from divalent metal ions behave as 1:2 electrolytes.[39]

The magnetic moments of the L-bisp complexes that contain paramagnetic metal ions, measured in the solid state at room temperature, indicate that the complexes are high spin. The values of μ_{eff} found for the cobalt(II)- and iron(II)-L-bisp complexes fall in the lower range usually observed for high-spin complexes[40] and are consistent with the presence of five-coordinate structures. These complexes apparently maintain the high-spin configuration in solution, since their proton NMR spectra recorded in CD_3CN solution at room temperature show large paramagnetic shifts, with chemical shift dispersions as high as 80–100 ppm. No ESR signal is exhibited by [Co(L-bisp)][ClO_4]$_2$ and [Fe(L-bisp)][ClO_4]$_2$, either in the solid state or in frozen solutions down to −150 °C. The ESR spectra of [Cu(L-bisp)][ClO_4]$_2$ recorded in frozen solutions suggest a pseudotetragonal site symmetry for the copper ion ($g_\parallel > g_\perp$, large $A_\parallel$ values). The spectrum recorded in frozen methanol solution (−150 °C) is better resolved than that in acetonitrile and gives $g_\parallel$ = 2.231 and $A_\parallel$ = 177 10^{-4} cm^{-1}. The high-field component of the signal is somewhat broadened, and the corresponding g values cannot be accurately determined from the spectrum. The unresolved anisotropy of the "in-plane" components indicates that the actual symmetry of the complex is probably intermediate between square pyramidal and trigonal bipyramidal, though closer to the tetragonal limit.[41]

The electronic spectrum of [Zn(L-bisp)][ClO_4]$_2$ dissolved in acetonitrile displays intense absorption bands near 300, 240, and 210 nm attributable to $\pi \rightarrow \pi^*$ transitions originating mainly within the trimethine unit of the ligand. Of these, the lowest energy transition can be assumed to be mostly localized within the imine groups, while the others are more typically pyridine ring transitions. The UV spectra of the other complexes with divalent metal ions are similar to that of [Zn(L-bisp)]$^{2+}$, while for [Cu(L-bisp)]$^+$ the lowest energy UV band is slightly blue shifted to 260 nm. In the visible region the spectrum of [Cu(L-bisp)]$^+$ shows two intense bands near 560 and 375 nm that we assume result from charge-transfer transitions from the filled copper(I) d orbitals to low-energy π^* orbitals of the ligand trimethine group. The visible spectrum of [Fe(L-bisp)]$^{2+}$ is also dominated by a strong absorption band near 500 nm. The apparent intensity of this band is too large for d–d transitions, and it is therefore assigned as a charge-transfer band, while the weak shoulders on the low-energy tail of the visible band possibly originate from d–d transitions. The visible spectrum of [Co(L-bisp)]$^{2+}$ displays only bands of low intensity, since the charge-transfer transitions apparently occur in the near-UV region, with an additional weak, broad, and featureless absorption band in the near-IR region. Bands of comparable intensities near the positions observed here for [Co(L-bisp)]$^{2+}$ have been assigned previously to high-spin, five-coordinate cobalt(II) complexes,[40a,42] in equilibrium with pseudooctahedral six-coordinate adducts in donor solvents.[42b] The visible spectrum of the brown [Cu(L-bisp)]$^{2+}$ complex shows only shoulders near 600, 450, and 350 nm on the low-energy tail of the intense UV band.

The CD spectra of [Zn(L-bisp)]$^{2+}$ and [Co(L-bisp)]$^{2+}$ reveal more detail than the corresponding absorption spectra, since

(37) Nakamoto, K. "Infrared and Raman Spectra of Inorganic and Coordination Compounds", 3rd ed.; Wiley-Interscience: New York, 1978.

(38) The CD_3CN NMR spectrum of [Cu(L-bisp)]$^+$ remains completely unchanged when the sample is heated to 50 °C. This seems to exclude the presence of conformational isomers in equilibrium in solution. The proton NMR spectrum of [Cu(L-bisp)]$^+$ in pyridine-d_5 shows the presence of two equally intense signals for the methyl ester (at δ 3.76 and 3.80) and CH_3C=N groups (at δ 2.37 and 2.44), while the pyridine-d_5 NMR spectrum of [Zn(L-bisp)]$^{2+}$ shows single signals for these groups (at δ 3.7 and 2.78, respectively). We have been unable to separate the copper(I) isomers, and fractional crystallization of [Cu(L-bisp)][ClO_4] from methanol under nitrogen gave optically inactive products with identical IR, UV, and NMR spectra.

(39) Geary, W. J. *Coord. Chem. Rev.* **1971**, *7*, 81–122.

(40) See, for instance: (a) Chen, Y.-Y.; Chu, D. E.; McKinney, B. D.; Willis, L. J.; Cummings, S. C. *Inorg. Chem.* **1981**, *20*, 1885–1892. (b) Niswander, R. H.; Martell, A. E. *Ibid.* **1978**, *17*, 2341–2344. (c) Busch, D. H.; Zimmer, L. L.; Grzybowski, J. J.; Olszanski, D. J.; Jackels, S. C.; Callahan, R. C.; Christoph, G. G. *Proc. Natl. Acad. Sci. U.S.A.* **1981**, *78*, 5919–5923. (d) Gullotti, M.; Casella, L.; Pasini, A.; Ugo, R. *J. Chem. Soc., Dalton Trans.* **1977**, 339–345. (e) Barefield, E. K.; Busch, D. H.; Nelson, S. M. *Q. Rev., Chem. Soc.* **1968**, *22*, 457–498.

(41) (a) Bencini, A.; Bertini, I.; Gatteschi, D.; Scozzafava, A. *Inorg. Chem.* **1978**, *17*, 3194–3197. (b) Bertini, I.; Scozzafava, A. *Met. Ions Biol. Syst.* **1981**, *12*, 31–74.

(42) (a) Sacconi, L.; Bertini, I. *J. Am. Chem. Soc.* **1966**, *88*, 5180–5185. (b) Boge, E. M.; Freyberg, D. P.; Kokot, E.; Mockler, G. M.; Sinn, E. *Inorg. Chem.* **1977**, *16*, 1655–1660.

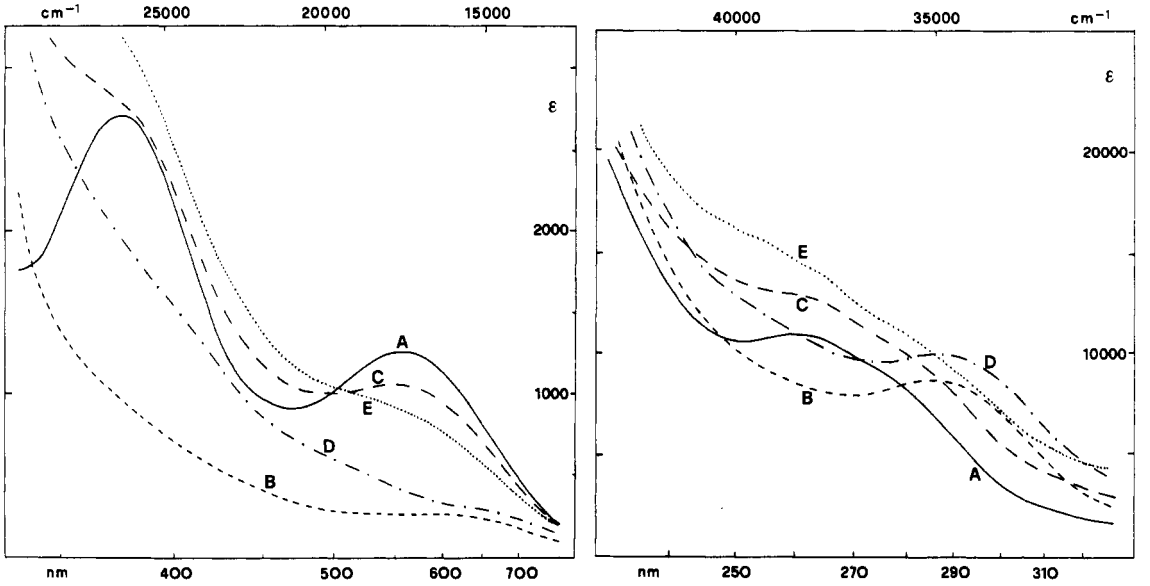

Figure 8. Electronic spectra of (A, —) [Cu(L-bisp)][ClO_4] in deoxygenated CH_3CN (concentration 5.6 × 10^{-4} M), (B, - - -) solution A after oxygenation (1 atm) for ca. 1 h at room temperature, (C, – –) solution B after degassing–gentle heating under N_2 for ca. 1 h, (D, –·–·) solution C after oxygenation for ca. 40 min, and (E, ···) solution D after a second oxy–deoxy cycle.

bands that occur as poorly defined shoulders in electronic spectra are often clearly resolved in CD spectra. We note that the sign of the CD bands of $[Co(L\text{-bisp})]^{2+}$ in the UV region, as well as that of the residual CD activity of $[Cu(L\text{-bisp})]^{2+}$ in the UV region (both negative) is that exhibited by $[Zn(L\text{-bisp})]^{2+}$. This probably reflects a similar conformation of the ligand in solution. A negative CD activity within the band associated with the $\pi \rightarrow \pi^*$ imine transition in the CD spectra of a variety of simple complexes of L-amino acid Schiff bases (including histidine, when bound like glycine) has been related to the preference for a λ conformation of the amino acid chelate ring.[16] As shown by the structure of $[Zn(L\text{-bisp})]^{2+}$, both chelate rings of the L-histidine residues display a conformation chirality of sign λ in the solid state. Therefore, we relate the CD features of $[Zn(L\text{-bisp})]^{2+}$, $[Co(L\text{-bisp})]^{2+}$, and $[Cu(L\text{-bisp})]^{2+}$ to the preference for a λ conformation of the chelate rings of the L-histidine residues in solution. This contrasts with the behavior exhibited by simple complexes of L-histidine Schiff bases in which the amino acid residue is bound like histamine, since these invariably show the preference for a δ conformation of the L-histidine chelate ring.[16c,d] However, in the latter complexes the imidazole ring occupies a coordination position coplanar with that of the imine group, and the carboxyl or carboxymethyl groups of the L-histidine residues are free to adopt the pseudoaxial disposition that involves a δ conformation of the amino acid chelate ring. For $[Zn(L\text{-bisp})]^{2+}$ this conformational arrangement is apparently no longer available since the imidazole rings are bound to the metal almost perpendicularly to the plane containing the zinc(II)–trimethine unit, and the adoption of a δ conformation by the L-histidine chelate rings would lead to significant steric interaction between the pseudoaxial carboxymethyl groups and the imidazole rings.

The collective structural, magnetic, and spectral evidence suggests that these L-bisp complexes in solution are five-coordinate, eventually in equilibrium with six-coordinate species, with the possible exception of $[Cu(L\text{-bisp})]^+$, for which an additional structure in which only four donor atoms of the ligand are bound to the metal cannot be completely eliminated.

Oxygenation of the Copper(I), Cobalt(II), and Iron(II) Complexes. It has been recently reported[17] that the complex $[Cu(imep)]^+$ reacts reversibly with molecular oxygen under ambient conditions. However, the compound isolated contained some impure paramagnetic material and so very little characterization of this copper(I) complex was given. It was therefore of some interest to investigate the reactivity of $[Cu(L\text{-bisp})]^+$ toward dioxygen since these copper(I) complexes probably have a very similar structure.

The complex [Cu(L-bisp)][ClO_4] does not react with dioxygen in the solid state and can be handled without any special precaution. Exposure to dioxygen (1 atm) of solutions of [Cu(L-bisp)][ClO_4] in deoxygenated, dry acetonitrile at room temperature results in the disappearance of the original violet color and yields a green solution. The reaction is complete in ca. 1 h and can be slowly reversed by degassing (N_2) and gentle heating of the oxygenated solution under a stream of dry nitrogen. The degree of reversibility of the reaction, determined spectrophotometrically, is about 80% and the oxy–deoxy cycling process can be repeated several times with approximately the same degree of reversibility for each successive cycle, until the solution becomes brown and does not show any color change with further exposure to dioxygen. If the solvent is not carefully dried, or if a protic solvent such as methanol is used, the oxygenation of [Cu(L-bisp)][ClO_4] is completely irreversible. The $[Cu(L\text{-bisp})]^+$ cation, therefore, behaves as its parent copper(I) complex derived from histamine,[17] although a qualitative comparison of reactivity under similar experimental conditions (see caption of Figure 8 for $Cu(L\text{-bisp})^+$ and caption of Figure 6 in ref 17b for $Cu(imep)^+$) shows that the oxygenation of $Cu(L\text{-bisp})^+$ occurs at a slower rate. Possibly the carboxymethyl groups of L-bisp lower the overall basicity of the ligand and lead to some increase of stability of the Cu(I) state. The spectral changes that occur upon oxygenation of [Cu(L-bisp)][ClO_4] are displayed in Figure 8. The absorption spectrum of $[Cu(L\text{-bisp})]^+$ in acetonitrile (A) shows two moderately intense charge-transfer bands in the visible region at 563 (ϵ 1250) and 376 nm (2700), while an intense band at 260 nm (ϵ 11 000) with a shoulder near 275 nm (9000) dominates the UV region. Oxygenation of solution A leads to spectrum B, which is almost featureless in the visible region with a broad band roughly centered at 600 nm and a poorly defined shoulder near 400 nm but which shows a red shift to ~290 nm of the UV band. This mostly intraligand transition has therefore undergone a shift to a position similar to those observed for the L-bisp complexes with divalent metal ions. Deoxygenation of solution B with N_2 and gentle heating for ca. 1 h generates spectrum C, which shows several features typical of the original $[Cu(L\text{-bisp})]^+$ complex.

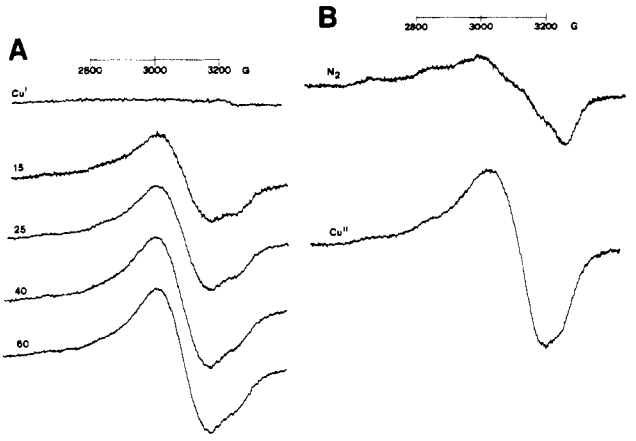

Figure 9. (A) ESR spectra at −130 °C of frozen acetonitrile solutions of [Cu(L-bisp)][ClO_4] (5.6×10^{-4} M) recorded after different times (in min) of oxygenation (ν 9.073 GHz). (B) ESR spectra of frozen acetonitrile solutions of [Cu(L-bisp)][ClO_4], as above after deoxygenation (first oxy–deoxy cycle), and of [Cu(L-bisp)][ClO_4]$_2$ in acetonitrile (identical concentration, ν 9.060 GHz).

In particularly, besides the reappearance of the visible bands near 560 and 380 nm, the UV maximum undergoes a reverse shift to ca. 260 nm. Spectra D and E result from a second oxy–deoxy cycling of solution C and again display features both in the visible and UV regions that are typical for solutions B and C, respectively. The reaction of [Cu(L-bisp)]$^+$ with dioxygen in acetonitrile was also followed by recording EPR spectra of the frozen solutions at different times of the oxygenation (Figure 9A). The intensity of the EPR signal increases during the oxygenation but is significant even at the early stages of the reaction. This was confirmed by unsuccessful attempts to follow the oxygenation of [Cu(L-bisp)]$^+$ in CD_3CN by NMR spectroscopy, where paramagnetic species were also formed. Figure 9B compares the EPR spectrum of the deoxygenated solution with that of a solution of [Cu(L-bisp)][ClO_4]$_2$ in acetonitrile with identical concentration. The amount of EPR-detectable copper in the deoxygenated solution is clearly lower than that available, and the features of its EPR signal are clearly different from those of both [Cu(L-bisp)]$^{2+}$ and the oxygenated solution.

In a series of experiments carried out under comparable conditions we have established that the degree of reversibility of the oxygenation of [Cu(L-bisp)]$^+$ (determined spectrophotometrically) is somewhat dependent on the rate at which the oxygenated solution is degassed and then warmed under the nitrogen stream. Aging of the oxygenated solution leads to a significant reduction in the extent of reversibility of the reaction. Moreover, the degree of reversibility of ~80% shown in Figure 8 represents an upper limit that seems dependent for instance on the initial concentration of [Cu(L-bisp)]$^+$ and therefore on eventual traces of impurities contained in the solvent. Manometric measurements show that a continuous, slow uptake of dioxygen takes place in solution. However, the amount of O_2 absorbed when the initial violet solution of [Cu(L-bisp)]$^+$ is converted into the oxygenated green solution (spectrum B in Figure 8, 30–40 min when oxygen-saturated solvent is used) is reproducible from sample to sample and corresponds to an uptake of 0.5 mol (±10%) of O_2 per copper. Thus the stoichiometry of the oxygenation reaction of [Cu(L-bisp)]$^+$ is the same as that found for [Cu(imep)]$^+$.[17] If exposure to dioxygen of the green solution is maintained, its color slowly changes to brown while the O_2 uptake continues slowly (about 1 mol of O_2/copper after 3–4 h). The electronic spectrum of this brown solution is very similar to that obtained after a few oxy–deoxy cycles of [Cu(L-bisp)]$^+$.

We are aware that the spectral changes undergone by [Cu(L-bisp)]$^+$ during the oxy–deoxy cycling may result from some ligand oxidation reaction or some cyclical oxidation to copper(II) followed by re-reduction to copper(I) in the absence of O_2 without necessarily involving an oxygen adduct. However, it must be noted that the oxygenation product of [Cu(L-bisp)]$^+$ is not simply [Cu(L-bisp)]$^{2+}$. This is evident from the ESR experiment in Figure 9 and is confirmed by the IR spectrum recorded of the green solid obtained upon slow evaporation to dryness of the cold green solution that results from the oxygenation of [Cu(L-bisp)]$^+$ in acetonitrile.[43] The spectrum is different from those of either [Cu(L-bisp)][ClO_4] or [Cu(L-bisp)][ClO_4]$_2$, for instance, the imine ν(C=N) band occurs at 1635 cm^{-1}, but shows that the functional groups of the ligand (ester and imine groups) are intact. It is obviously impossible to make any deductions about structure from IR data since the spectra of the various L-bisp complexes show significant differences in several regions. However, the weak band near 3550 cm^{-1}, which is absent in the IR spectrum of the starting [Cu(L-bisp)][ClO_4] complex, may be associated with the presence of hydroxide or hydroxyl groups,[13k,n,p,r] possibly resulting from cleavage of a supposed coordinated dioxygen species and proton abstraction from, for example, the imidazole NH groups of the ligand. Whether this band belongs to the initially oxygenated [Cu(L-bisp)]$^+$ complex or to the aged species is difficult to assess. The brown solid obtained upon evaporation to dryness of the irreversibly oxygenated [Cu(L-bisp)]$^+$ solution displays an IR spectrum very similar to that of the green material, except for the 650–800-cm^{-1} region, where additional weak bands occur at 658, 770, and 787 cm^{-1}.[44] This suggests that oxygenation of [Cu(L-bisp)]$^+$ occurs without concomitant extensive ligand destruction. Interestingly, when the green oxygenation product of [Cu(L-bisp)]$^+$ is heated in the mass spectrometer, the peak at m/e 32 corresponding to molecular oxygen increases remarkably in intensity up to a 1:1 ratio with respect to the N_2 peak at m/e 28 of the background air, while under exactly the same conditions the usual ratio of approximately 0.25:1 (±5%) between the peaks at m/e 32 and 28 is invariably observed for [Cu(L-bisp)][ClO_4]$_2$, [Cu(L-bisp)][ClO_4]$_2$, [Zn(L-bisp)][ClO_4]$_2$, and [Co(L-bisp)][ClO_4]$_2$ and also for the brown material that results from the irreversibly oxygenated solution of [Cu(L-bisp)][ClO_4].[45] These data are by no means quantitative but show that some simple copper–dioxygen adduct is probably present at the early stages of the oxygenation of [Cu(L-bisp)]$^+$.

While the reaction of molecular oxygen with cobalt(II) complexes generally produces relatively stable superoxo and μ-peroxo intermediates,[3] it is known, largely on the basis of studies on modified porphyrin complexes[46] and, more recently, on non-porphyrin macrocyclic complexes,[47] that stringent structural factors rule dioxygen binding by iron(II) model complexes.[48] Although the L-bisp ligand does not satisfy these

(43) Analytical data of the green material obtained upon oxygenation of [Cu(L-bisp)][ClO_4] are as follows. Anal. Calcd for the rough formula corresponding to [Cu(L-bisp)][ClO_4]·$^1/_2O_2$: C, 42.85; H, 4.22; N, 15.21. Found: C, 42.59; H, 4.26; N, 15.48. Complete IR data (Nujol mull, cm^{-1}): 3547 w, 3290 m, 3131 m, 1735 s, 1635 m, 1596 m, 1496 vw, 1316 vw, 1270 m, 1232 m, 1209 m, 1182 sh, 1160 w, 1097 vs, 1021 w, 963 w, 930 w, 852 w, 818 m, 752 w, 721 w, 695 w, 660 sh, 623 s.

(44) Analytical data of the brown material obtained upon extensive oxygenation of [Cu(L-bisp)][ClO_4] are as follows: Anal. Found: C, 41.93; H, 4.06; N, 15.44.

(45) The peak at m/e 32 occurs in the MS spectrum of [Fe(L-bisp)][ClO_4]$_2$·CH_3OH, but this arises from the release of methanol by the complex, as indicated by the intense fragmentation peaks at m/e 31 and 29.

(46) (a) Collman, J. P.; Gagné, R. R.; Reed, C. A.; Halbert, T. R.; Lang, G.; Robinson, W. T. *J. Am. Chem. Soc.* **1975**, *97*, 1427–1439. (b) Collman, J. P.; Gagné, R. R.; Halbert, T. R.; Marchon, J. C.; Reed, C. A. *Ibid.* **1973**, *95*, 7868–7870. (c) Almog, J.; Baldwin, J. E.; Huff, J. *Ibid.* **1975**, *97*, 227–228. (d) Traylor, T. G.; Campbell, D.; Tsuchiya, S. *Ibid.* **1979**, *101*, 4748–4749.

(47) Herron, N.; Busch, D. H. *J. Am. Chem. Soc.* **1981**, *103*, 1236–1237.

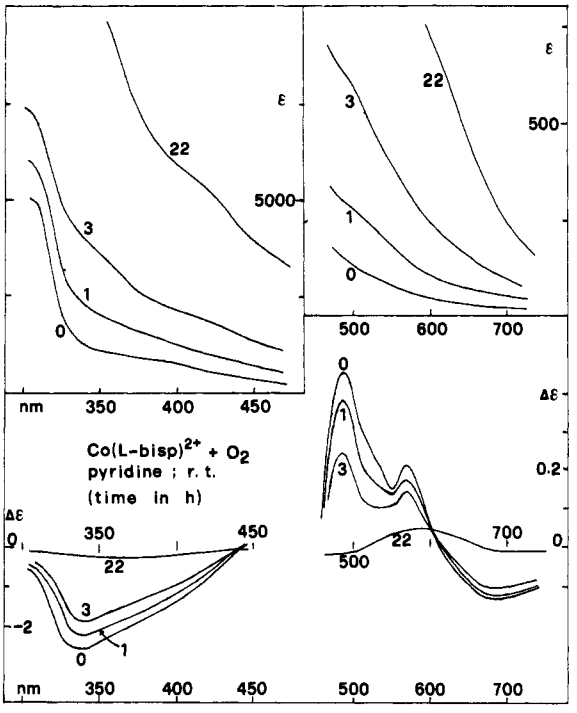

Figure 10. Electronic and CD spectra recorded at different times of the oxygenation (1 atm) of $[Co(L\text{-bisp})][ClO_4]_2$ in pyridine solution at room temperature (concentration 10^{-3} M). Spectral readings were taken after the time indicated (h).

structural requirements, we thought it of interest to compare the reactivity toward dioxygen of the copper(I), iron(II), and cobalt(II) complexes derived from the same ligand. Both $[Fe(L\text{-bisp})][ClO_4]_2$ and $[Co(L\text{-bisp})][ClO_4]_2$ are completely stable to oxidation in the solid state and exhibit extremely low or no reactivity toward dioxygen when dissolved in carefully dried, weakly basic solvents such as dimethylformamide or acetonitrile. But pyridine solutions of these complexes undergo slow reactions when exposed to dioxygen (1 atm) at room temperature. These reactions are not reversed by degassing and warming the solutions under a stream of dry nitrogen.[49] The spectral changes accompanying the reaction of $[Co(L\text{-bisp})]^{2+}$ with O_2 in pyridine are displayed in Figure 10. The pink-yellow color of the complex in pyridine slowly turns brown while dioxygen is absorbed by the solution, and a constant increase in intensity of the absorption spectrum is observed. Only additional ill-defined shoulders near 350 and 500 nm can be detected in the oxygenated solution. The observation of a CD spectrum during the oxygenation is made difficult by the concomitant racemization reaction of $[Co(L\text{-bisp})]^{2+}$ in pyridine (Figure 5), which occurs at a comparable rate. The only appreciable changes to be ascribed to the oxygenation reaction occur in the 500-nm region. Manometric measurements of the oxygen absorbed show that the uptake is slower than it is for $[Cu(L\text{-bisp})]^{+}$ (approximately 0.5 mol (±10%) of O_2/cobalt after 7 h, and 1.5 mol of O_2/cobalt after 2 days), while no ESR signal can be detected in the spectra recorded at different times on the frozen oxygenated solutions. Therefore, neither low-spin Co(II) nor ESR-active cobalt–dioxygen species apparently accumulate in solution during the oxygenation. We believe that the oxygenation product is diamagnetic, since the solid samples obtained after evaporation to dryness at different times show a progressive decrease in magnetic moment.[50] These solid samples release dioxygen when heated in the mass spectrometer, and their IR spectra in the region 700–930 cm^{-1} differ only slightly from those of the starting cobalt(II) complex.[51] In particular, upon oxygenation a weak band at 848 cm^{-1} disappears, the doublet near 745 cm^{-1} is replaced by a single band at 755 cm^{-1}, and only very weak new bands occur at 905 and 680 cm^{-1}. Although we cannot make reliable assignments of these bands, we note that weak IR bands in the range 740–930 cm^{-1} have been assigned to $\nu(O_2)$ in binuclear, diamagnetic "μ-peroxo" cobalt–dioxygen complexes.[52] The stoichiometry of oxygen binding, magnetism, and lack of ESR signal agree with this formulation for the oxygenation product of $[Co(L\text{-bisp})]^{2+}$. But the adduct is apparently kinetically labile, for when oxygenation of $[Co(L\text{-bisp})]^{2+}$ in pyridine is continued beyond approximately 24 h, the IR spectra of the resulting products clearly indicate a progressive alteration of the functional groups of the ligand, since the ester $\nu(C{=}O)$ band undergoes a reduction in intensity and new IR bands appear near 1700 and 1650 cm^{-1}. Note that these are not related to formation of 2,6-diacetylpyridine, which also shows a $\nu(C{=}O)$ band near 1700 cm^{-1}, since other characteristic IR bands of this compound (e.g. at 1360, 1301, and 1234 cm^{-1}) are absent in the spectra of the oxidation products. Also, hydrogen peroxide is not a product of the oxygenation of $Co(L\text{-bisp})^{2+}$, since qualitative tests with potassium iodide at different times of the oxygenation gave negative results.

The oxygenation of $[Fe(L\text{-bisp})]^{2+}$ in pyridine produces a marked increase of electronic absorption below ~450 nm, while the visible band near 550 nm undergoes a corresponding decrease in intensity (Figure 11).[27] The blue color of $[Fe(L\text{-bisp})]^{2+}$ in pyridine slowly turns brown during the oxygenation. Manometric measurements show that the uptake of dioxygen occurs at a faster rate than for $[Co(L\text{-bisp})]^{2+}$ (approximately 0.5 mol (±10%) of O_2 per iron after 2 h, and 1 mol of O_2 per iron after 4 h). The ESR spectra recorded in frozen solution at different times of the oxygenation show only the appearance of very weak signals near $g = 4.3$, 2.2, and 1.9 that probably arise from a minor amount of iron(III) species. It is likely that no simple iron–dioxygen species accumulates in solution, and the spectra in Figure 11 are not indicative of a simple equilibrium in solution. The solid material obtained upon evaporation to dryness of the oxygenated solution shows no release of dioxygen when heated in the mass spectrometer. Moreover, the IR spectra of these products show the presence of IR bands near 1700 and 1650 cm^{-1}, similar to those exhibited by the decomposition products of $[Co(L\text{-bisp})]^{2+} + O_2$. The products resulting from oxygenation for 24 h of $[Fe(L\text{-bisp})]^{2+}$ (approximately 2 mol of O_2/iron absorbed) display an IR spectrum with a broad band that extends from 1600 to 1750 cm^{-1} and is centered near 1650 cm^{-1}. Therefore, the oxygenation of $[Fe(L\text{-bisp})]^{2+}$, and partly of $[Co(L\text{-bisp})]^{2+}$, produces an apparent oxidation of the ligand. The ester and imino groups are probably involved in the oxidation reaction;

(48) Jameson, G. B.; Ibers, J. A. *Comments Inorg. Chem.* **1983**, *2*, 97–126.
(49) Note that the oxygenation of $[Cu(L\text{-bisp})][ClO_4]$ in pyridine is also irreversible.
(50) An adduct containing approximately two molecules of pyridine is obtained upon evaporation to dryness at room temperature of a pyridine solution of $[Co(L\text{-bisp})][ClO_4]_2$. Anal. Calcd for $C_{23}H_{27}CoCl_2N_7O_{12}\cdot 2C_5H_5N$: C, 44.96; H, 4.23; N, 14.30. Found: C, 45.95; H, 4.18; N, 14.53. This product has a magnetic moment of 4.21 μ_B, almost coincident with that of $[Co(L\text{-bisp})][ClO_4]_2$. The material isolated upon evaporation to dryness under vacuum at room temperature of a pyridine solution of $[Co(L\text{-bisp})][ClO_4]_2$ after oxygenation for approximately 20 h has a magnetic moment of 1.42 μ_B. Anal. Found: C, 44.89; H, 4.00; N, 13.91.
(51) Complete IR data of $[Co(L\text{-bisp})][ClO_4]_2\cdot 2C_5H_5N$, (Nujol null, cm^{-1}): 3275 w, br, 3126 w, 3080 w, 1735 s, 1623 m, 1585 s, 1496 w, 1325 w, 1272 m, 1240 w, 1203 m, 1172 m, 1090 s, br, 1028 s, 930 m, 889 vw, 848 w, 813 m, 750 m, 743 m, 704 m, 620 s.
(52) (a) Barraclough, C. G.; Lawrance, G. A.; Lay, P. A. *Inorg. Chem.* **1978**, *17*, 3317–3322. (b) Nakamoto, K.; Suzuki, M.; Ishiguro, T.; Kozuka, M.; Nishida, Y.; Kida, S. *Ibid.* **1980**, *19*, 2822–2824. (c) Suzuki, M.; Ishiguro, T.; Kozuka, M.; Nakamoto, K. *Ibid.* **1981**, *20*, 1993–1996.

the IR bands at 1650-1700 cm^{-1} observed in the spectra of the oxidation products are probably indicative of the formation of carbonyl groups. Products containing these functions have been shown to result from oxidation of the ligand by reaction of metal complexes with dioxygen.[53] It is important to note that the products that result from the irreversible oxygenation of $[Cu(L\text{-bisp})]^+$ are different, as the ester and imino groups of the ligand are unaffected. It is possible that in the Cu reaction the ligand undergoes simple hydroxylation, apparently a common route for the evolution of many Cu(I) + O_2 systems. The L-bisp ligand appears to provide some stabilization for simple copper-dioxygen and cobalt-dioxygen species formed at the early stages of the oxygenation. We are currently trying to characterize these species.

Acknowledgment. This work was supported by the Italian MPI and by the U.S. National Institutes of Health (Grant No. HL 13157). We thank the Italian CNR for instrumentation facilities, M. Bonfa for recording the NMR spectra, P. Russo for the MS spectra measurements, and M. S. Franzoni for the magnetic susceptibility measurements.

(53) Gözen, S.; Peters, R.; Owston, P. G.; Tasker, P. A. *J. Chem. Soc., Chem. Commun.* **1980**, 1199-1201 and references therein.

Registry No. $[Cu(L\text{-bisp})][ClO_4]$, 89196-41-8; $[Zn(L\text{-bisp})][ClO_4]_2$, 89178-90-5; $[Cu(L\text{-bisp})][ClO_4]_2$, 89178-92-7; $[Co(L\text{-bisp})][ClO_4]_2$, 89178-94-9; $[Fe(L\text{-bisp})][ClO_4]_2$, 89178-96-1; O_2, 7782-44-7; L-histidine methyl ester, 1499-46-3; 2,6-diacetylpyridine, 1129-30-2.

Supplementary Material Available: Listings of thermal parameters for the non-hydrogen atoms (Table III), idealized hydrogen positions (Table IV), observed and calculated structure amplitudes (Table V), bond distances and angles in the coordination sphere (Table VI), and least-squares planes (Table VII) and circular dichroism spectra of $[Co(L\text{-bisp})][ClO_4]_2$ in degassed pyridine at different times (Figure 5), proton NMR spectra of $[Cu(L\text{-bisp})][ClO_4]$ in degassed CD_3CN (Figure 6) and $[Zn(L\text{-bisp})][ClO_4]_2$ in CD_3CN (Figure 7), and electronic spectra in the oxygenation of $[Fe(L\text{-bisp})][ClO_4]_2$ (Figure 11) (29 pages). Ordering information is given on any current masthead page.

Contribution from the Ministero della Pubblica Istruzione of Italy, Istituto di Chimica Generale e Inorganica, University of Modena, 41100 Modena, Italy

Coordination Behavior of 4-Toluenesulfonamide Derivatives: Thermal and Spectroscopic Properties of (*N*-Tosylglycinato)(2,2'-bipyridine)copper(II) Complexes. Crystal and Molecular Structure of (Ethanol)(*N*-tosylglycinato)(2,2'-bipyridine)copper(II)

L. ANTOLINI and L. MENABUE*[1]

Received April 20, 1983

The compounds of formula [Cu(Tsgly)(bpy)L] and anhydrous [Cu(Tsgly)(bpy)] (Tsgly = *N*-tosylglycinate dianion; bpy = 2,2'-bipyridine; L = EtOH, H_2O) were synthesized and characterized by means of thermogravimetric, electronic, infrared, and EPR spectra. For one of them, the [Cu(Tsgly)(bpy)(EtOH)] complex, the crystal structure was also determined. The compound crystallizes in the monoclinic space group $P2_1/n$ with 4 formula units in a cell of dimensions a = 9.677 (1) Å, b = 10.460 (1) Å, c = 21.488 (2) Å, and β = 98.27 (1)°. The structure was solved by the heavy-atom method and refined by least-squares calculations to R = 0.039 for 1705 observed reflections. The structure consists of discrete molecular units of [Cu(Tsgly)(bpy)(EtOH)]. The Cu atom shows tetrahedrally distorted square-pyramidal N_3O_2 coordination. The Tsgly dianion and the bpy molecule act as bidentate ligands in the equatorial plane, and the ethanol is bonded to the metal atom in the apical position. The thermogravimetric, EPR, and electronic results for the aquo and ethanol derivatives suggest that the stability of the in-plane ligands permits successive substitution reactions at the apical position. The infrared spectra for the aquo and ethanol adducts are consistent with the presence of a coordinated water or ethanol molecule.

Introduction

Investigation of the Cu(II)-*N*-tosylglycinate system in the solid state and in solution (aqueous and ethanolic)[2] has pointed out, on the one hand, the differences in the coordination behavior of this *N*-tosyl derivative with respect to that of *N*-acetyl and *N*-benzoyl ones[3] and, on the other hand, some meaningful similarities with the pH-dependent coordination behavior of oligoglycines.[4] In fact in these peptides and in *N*-tosylglycine,[2,4] contrary to *N*-acetyl and *N*-benzoyl derivatives,[3] the presence of the Cu(II) ion enables the deprotonation of the peptide or sulfonamide nitrogen atom. As a consequence, the *N*-tosylglycine may act as a bidentate ligand through a carboxylic oxygen atom and the deprotonated sulfonamide nitrogen atom, forming a very stable five-membered chelate ring. In fact at pH ≥ 5 it separates the complex $[Cu(Tsgly)(H_2O)_3]$ where the copper(II) ion is in a square-pyramidal arrangement.[2a] As this aquo complex contains three coordinated water molecules,[2a] it must easily react with nitrogen donor ligands. Therefore, in this paper we report the structural, spectroscopic, and thermogravimetric results on the ternary complexes obtained by reaction of $[Cu(Tsgly)(H_2O)_3]$ with bpy (2,2'-bipyridine) in ethanolic and aqueous solution with the aim of

(1) To whom correspondence should be addressed.

(2) (a) Antolini, L.; Battaglia, L. P.; Battistuzzi Gavioli, G.; Bonamartini Corradi, A.; Grandi, G.; Marcotrigiano, G.; Menabue, L.; Pellacani, G. C. *J. Am. Chem. Soc.* **1983**, *105*, 4327 (Part 1). (b) *Ibid.* **1983**, *105*, 4333 (Part 2). (c) *Inorg. Chim. Acta* **1983**, *79(B7)*, 262. (d) Battaglia, L. P.; Bonamartini Corradi, A.; Marcotrigiano, G.; Menabue, L.; Pellacani, G. C. *Inorg. Chem.* **1983**, *22*, 1902 (Part 3). (e) Battaglia, L. P.; Bonamartini Corradi, A.; Menabue, L. *Ibid.* **1983**, *22*, 3251. (f) Fenyo, J. C.; Beaumais, J.; Selegny, E.; Petit-Ramel, M.; Martin, R. P. *J. Chem. Phys.* **1973**, 299.

(3) See for example: (a) Marcotrigiano, G.; Pellacani, G. C.; Battaglia, L. P.; Bonamartini Corradi, A. *Cryst. Struct. Commun.* **1976**, *5*, 923. (b) Udupa, M. R.; Krebs, B. *Inorg. Chim. Acta* **1978**, *31*, 258. (c) *Ibid.* **1979**, *37*, 1. (d) Brown, J. N.; Eichelberger, H. R.; Schaeffer, E.; Good, M. L.; Trefonas, L. M. *J. Am. Chem. Soc.* **1971**, *93*, 6390. (e) Battaglia, L. P.; Bonamartini Corradi, A.; Marcotrigiano, G.; Menabue, L.; Pellacani, G. C. *J. Am. Chem. Soc.* **1980**, *102*, 2663. (f) *Inorg. Chem.* **1981**, *20*, 1075. (g) Antolini, L.; Battaglia, L. P.; Bonamartini Corradi, A.; Marcotrigiano, G.; Menabue, L.; Pellacani, G. C.; Saladini, M. *Ibid.* **1982**, *21*, 1391. (h) Battaglia, L. P.; Bonamartini Corradi, A.; Menabue, L.; Pellacani, G. C.; Prampolini, P.; Saladini, M. *J. Chem. Soc., Dalton Trans.* **1982**, 781.

(4) (a) Freeman, H. C. *Adv. Protein Chem.* **1967**, *22*, 257. (b) Bell, J. D.; Freeman, H. C.; Wood, A. M.; Driver, R.; Walker, W. R. *J. Chem. Soc., Chem. Commun.* **1969**, 1441. (c) Margerum, D. W.; Dukes, G. R. *Met. Ions Biol. Syst.* **1974**, *1*, 157. (d) Freeman, H. C. *Inorg. Biochem.* **1974**, *1*, 121 and references cited therein. (e) Lim, M. C.; Sinn, E.; Martin, R. B. *Inorg. Chem.* **1976**, *15*, 807. (f) Dehand, J.; Jordanov, J.; Keck, F.; Mosset, A.; Bonnet, J. J.; Galy, J. *Inorg. Chem.* **1979**, *18*, 1543.

0020-1669/84/1323-1418$01.50/0